



Intense non-linear soft x-ray emission from a hydride target during pulsed D bombardment

G.H. Miley¹, A.G. Lipson^{1, 2}, W. Helgeston⁴, H. Hora⁵, N. Luo¹, Y. Yang¹, M. Romer¹, R. Smith³

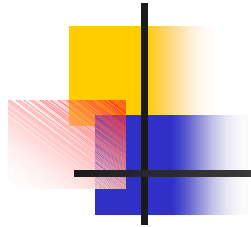
1 University of Illinois at Urbana-Champaign, Dept. Nuclear, Plasma & Radiological Engineering, 103 S. Goodwin Ave. Urbana, IL, 61801 USA. ghmiley@uiuc.edu

2 Institute of Physical Chemistry, The Russian Academy of Sciences, Moscow 119915, Russia

3 Oakton International Corporation, Oakton, VA 22124

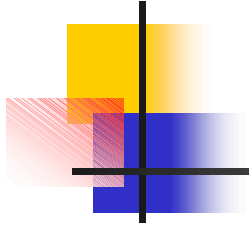
4 New Mexico Tech-IERA, 901 University Blvd S.E., Albuquerque, NM 87106-4339

5 Dept. of Theoretical Physics, Univ. of New South Wales, Sydney, 2052, Australia



Outline

1. Goal
2. Background – prior work
3. Initial results
 1. Experimental
 2. Theory
4. Summary



Goal

- Gain understanding of soft xray emission during pulsed GD plasma bombardment of hydrides.
- Long term
 - Compact coherent soft xray source in keV range.
 - Study other phenomena uoccuring under pulsed GD conditions, e.g. transmtations, excess power...



Background

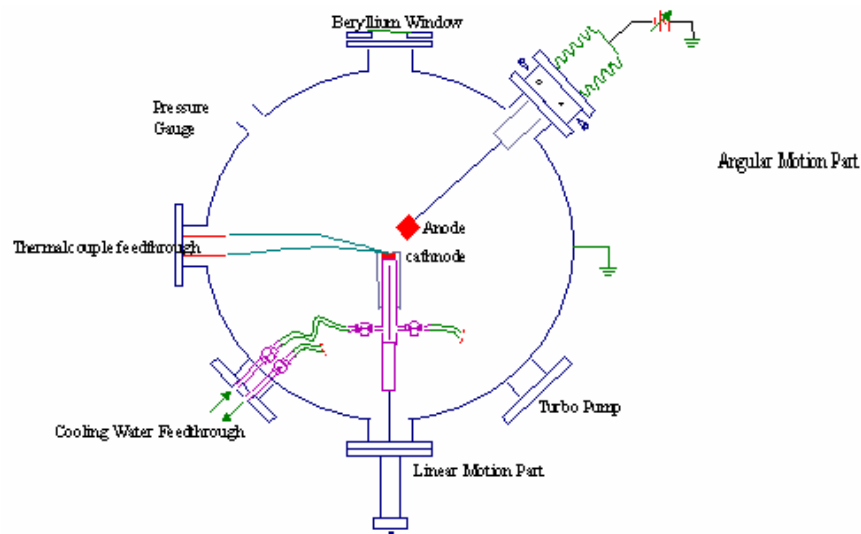
- Prior studies by A. Karabut, Lutch Lab, Moscow suggest coherent xray emission possible with GD bombardment of targets.
- UIUC experiments – initially concentrate on sub-threshold x-ray emission using a modified, large volume discharge set-up.



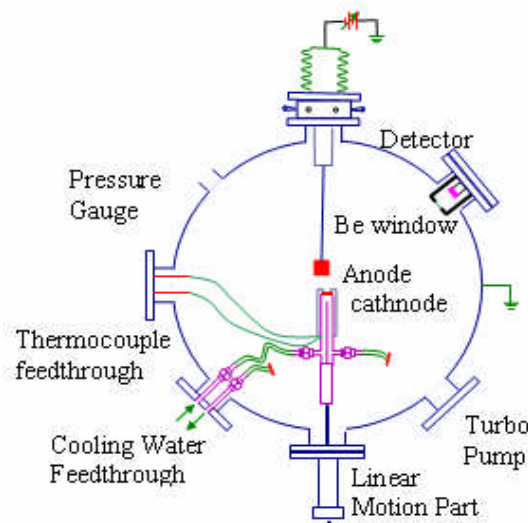
Initial Work

- Designed and set up flexible large volume discharge device for study
- Built specialized pulsed power supply to cover a range of pulse shapes and rep rates
- Set up film and solid state detector array
- Carried out initial experiments demonstrating operation and anomalous x-ray emission.
- Performed auxiliary x-ray measurements during room T desorption.

The large volume UIUC chamber gives room for internal diagnostics. Also the anode cathode separation is easily adjusted. A photo of the discharge is also shown.



Internal Layout



- A positive voltage is applied at the anode. Cathode and vessel are grounded.
- A plasma is produced between this and the water-cooled cathode.
- Cathode on movable mount to vary electrode spacing.
- The G-D plasma is covered by glass cylinder.
- The photodiode uses a thin Beryllium filter for energy resolution.
- Roughing Pump and Deuterium gas pipe regulate pressure.

Photo of setup

- The experiment is housed in a spherical vacuum chamber
- 10 smaller ports
 - Measurements and inputs
- 4 larger ports
 - Pumping and view ports



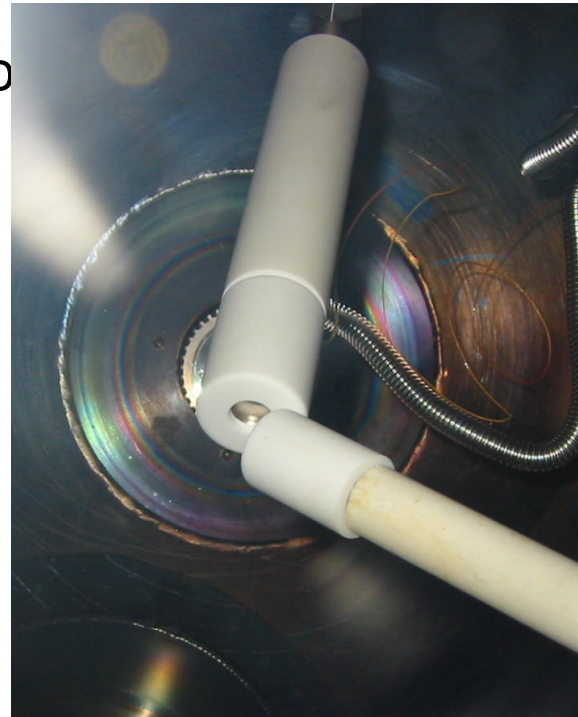
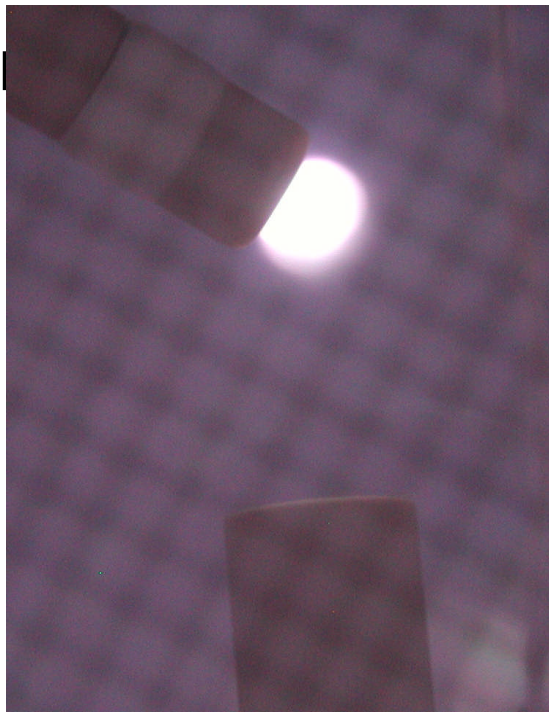


Electrodes have flexible design:

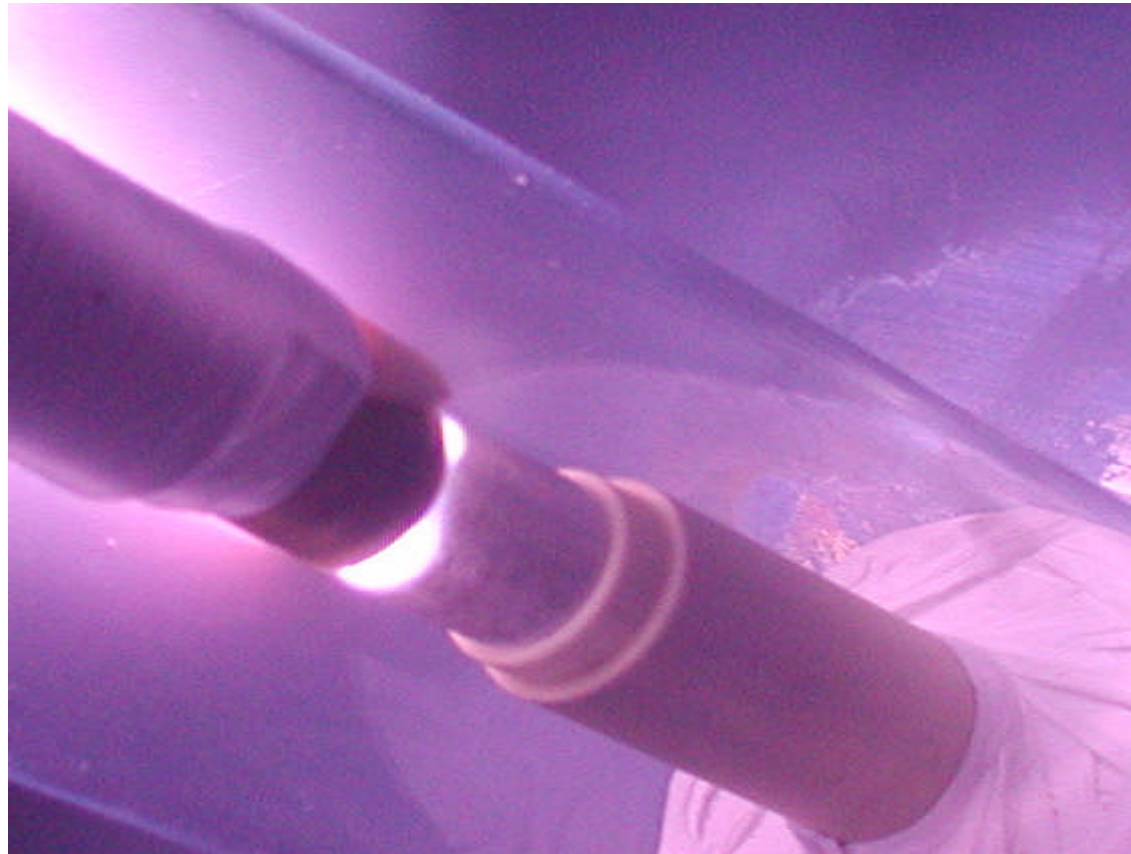
Water-cooling cathode (Target can be mounted easily, capable of linear motion).

Stainless steel anode (Capable of angular motion).

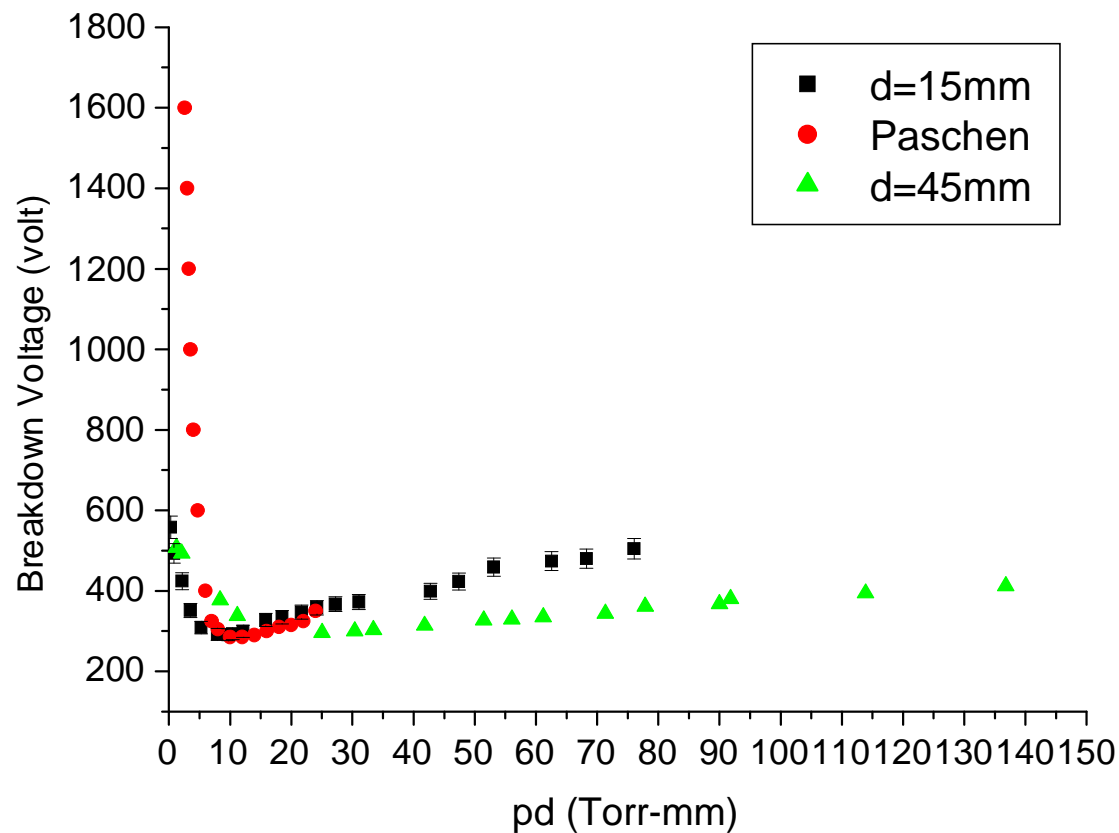
K type thermocouple embedded between the target and the water-cooling jacket.



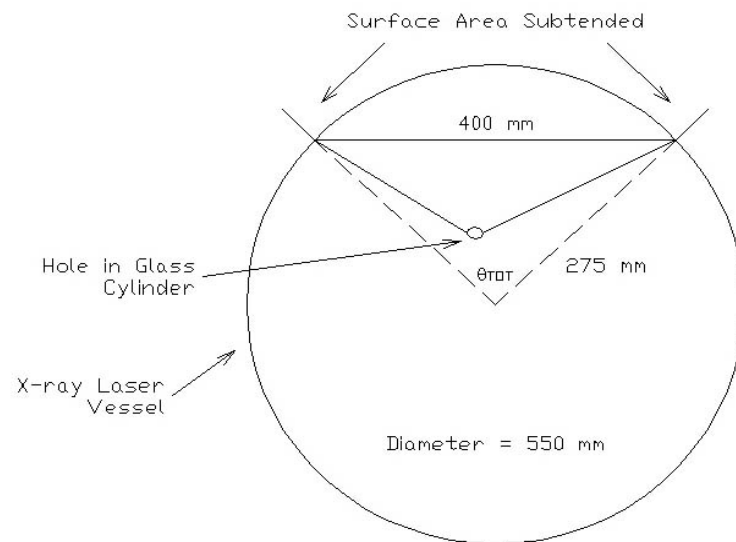
Discharge with parallel arrangement (used for data given here) – glass tube added around discharge to prevent stray breakdown



Ideal Paschen curve and the $V \sim pd$ curve for basic configuration

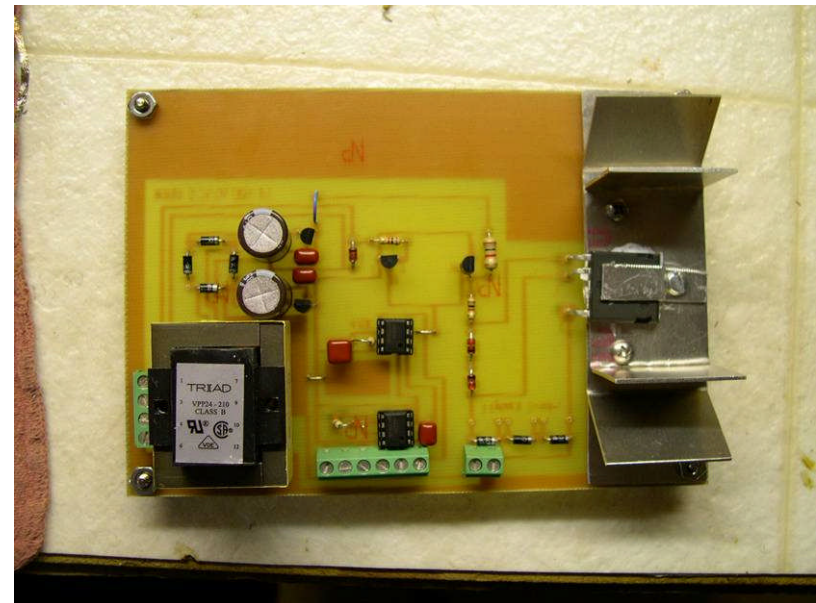


Internal Geometry

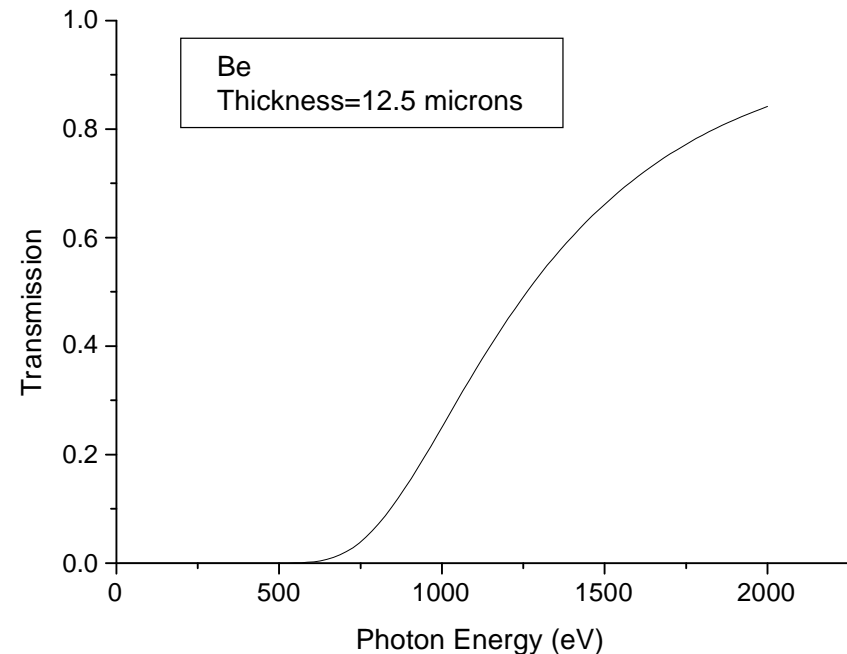
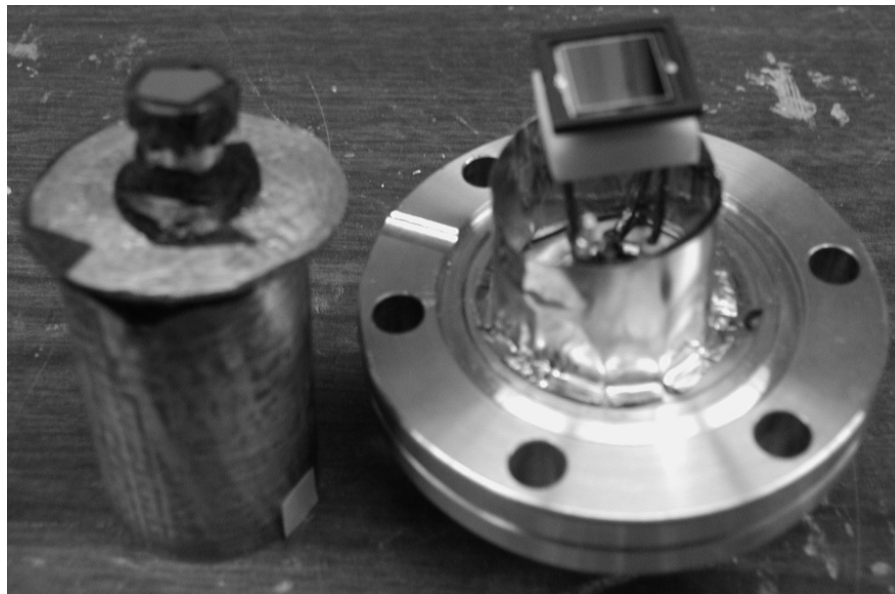


- The chamber is a sphere of radius 275 mm.
- The X-rays are emitted from the surface of the cathode and are blocked by a glass cylinder.
- They arrive at a reduced section of the spherical chamber that forms a solid angle of about 1.73 Steradians.

The 2.2 kVA power supply is shown below. The circuit board controlling the frequency is working well for values of 100 Hz to 1800 Hz and the pulse width modulation works well with duty cycles of 5% to 95%.

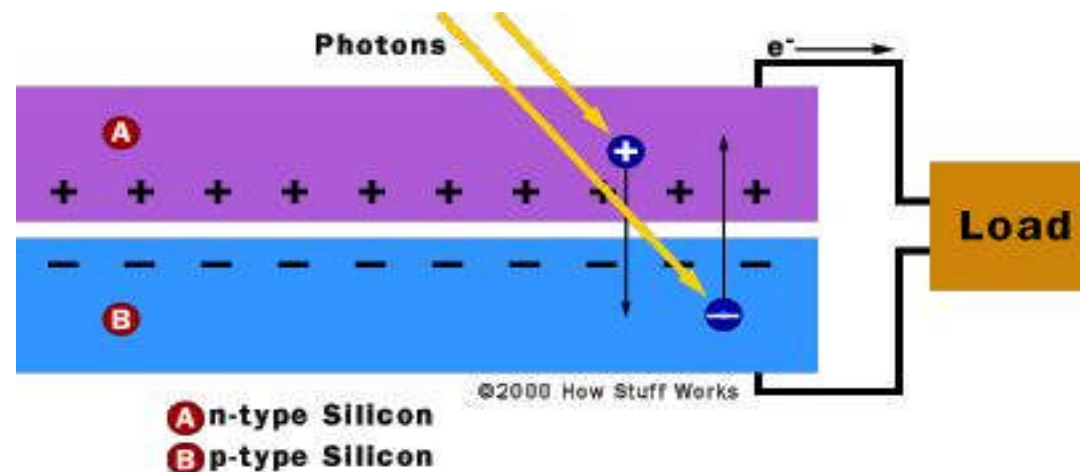


The AXUV photodiode detector (right) and the beryllium filter (left) are shown below. The filter's purpose is to prevent the visible light from the glow discharge from reaching the detector. The filter transmission curve is on the far right – note that x-rays of < 600 eV are cut off.



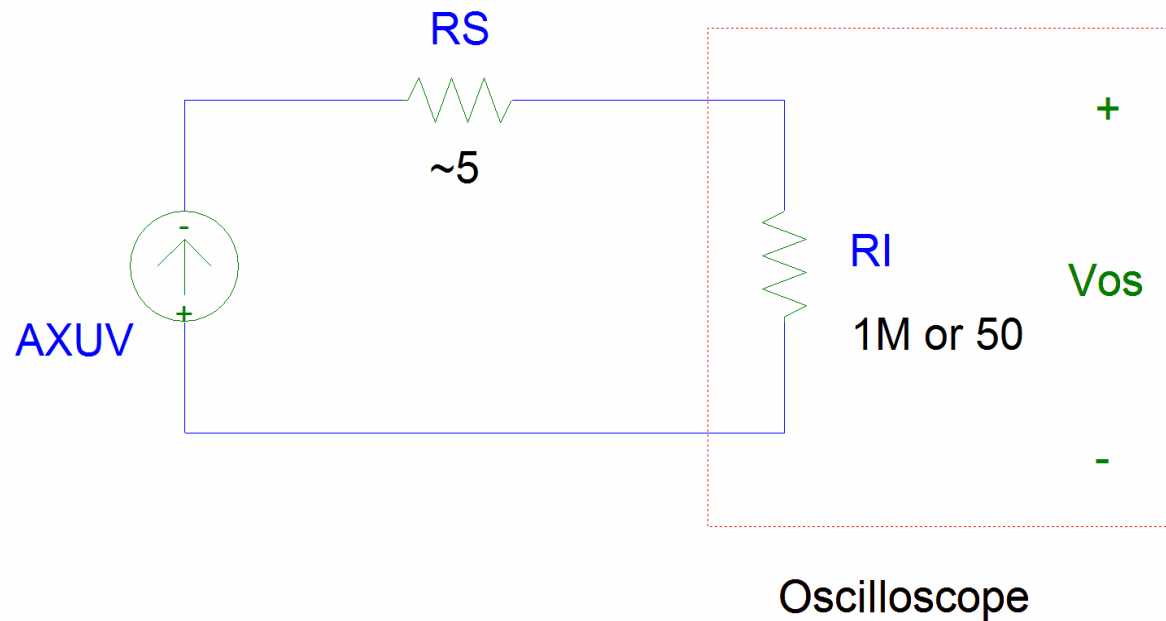
Radiation Detector Operation

- p-n Junction Diode
- Electron-Hole Pairs Formed in depletion volume
- Surface window thickness minimized for soft x-rays
- Be filters used for energy determination



Equivalent Circuit

- Radiation Detector and Oscilloscope
- Variable Oscilloscope Resistance



Oscilloscope Operational Data – low resistance generally used for fast rise time

Parameter	Symbol	Units	Value
Series Resistance	R_S	Ω	5
Oscilloscope Low Input Resistance	R_{I-Low}	Ω	50
Oscilloscope High Input Resistance	R_{I-High}	Ω	10^6
Photodiode Capacitance	C	pF	4
Fraction of Measured Current (R_{I-Low})	$f_{I-50\Omega} = \frac{R_{I-Low}}{R_{I-Low} + R_S}$		0.91
Fraction of Measured Current (R_{I-High})	$f_{I-1M\Omega} = \frac{R_{I-High}}{R_{I-High} + R_S}$		~ 1.00
Rise Time (R_{I-Low})	$\tau_{50\Omega} = 2.2(R_S + R_{I-Low})C$	s	0.48×10^{-9}
Rise Time (R_{I-High})	$\tau_{1M\Omega} = 2.2(R_S + R_{I-High})C$	s	8.8×10^{-6}



AXUV Photodiode Calibration

- A carbon-14 beta particle source was used to calibrate the AXUV photodiode radiation detector
- The responsivity of the expected 1-2 keV photons is very similar to the AXUV responsivity for 50 keV (average) carbon-14 betas
- The carbon-14 source was applied to the photodiode detector with all external lighting turned off, and the output was measured on an oscilloscope
- The resulting oscilloscope voltage induced by the carbon-14 was near the expected value, and the calibration was deemed successful

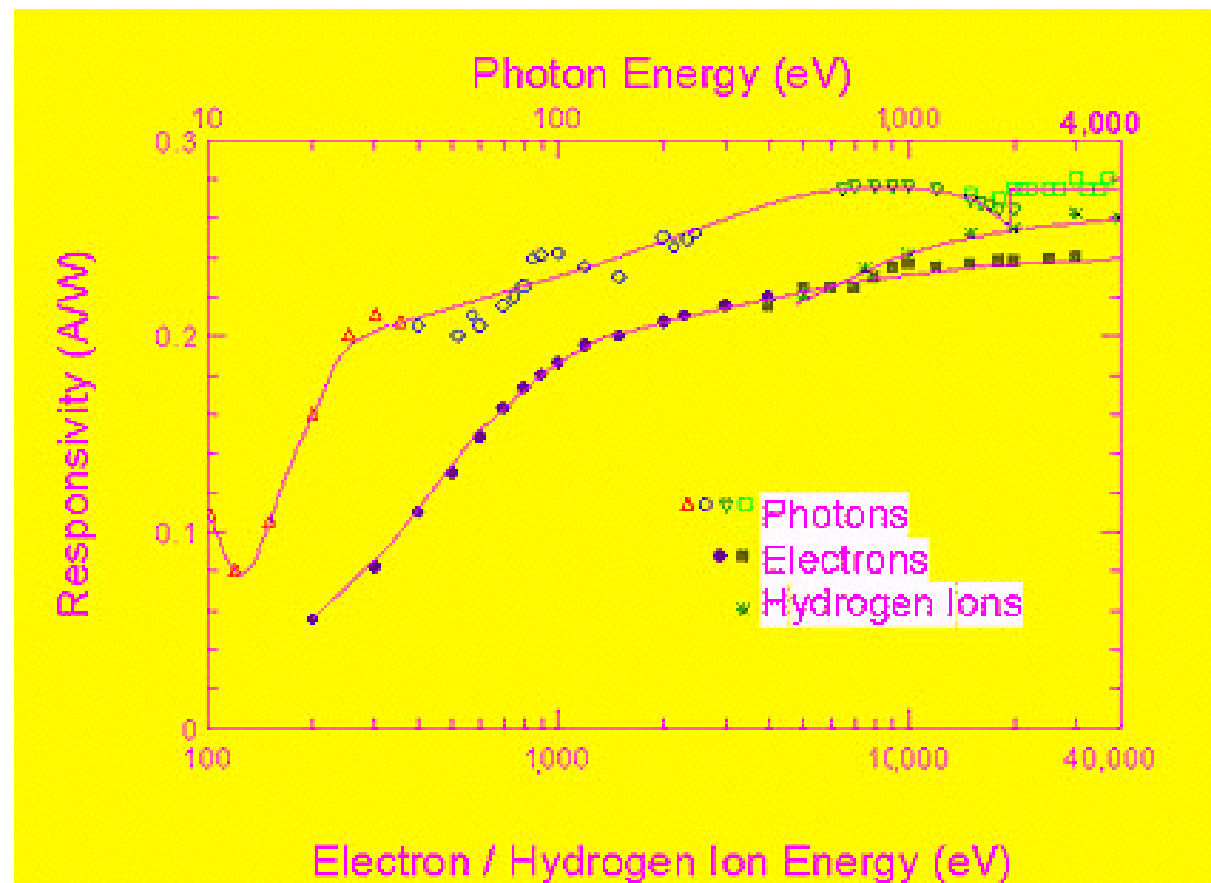
Detector Calibration

- C-14 Source (7.5 mCi)
- $\beta_{\text{avg}} = 49.5 \text{ keV}$
- Reasonable simulation for soft x-rays



ICCF- 12 2005

Not all of the radiation energy that enters the AXUV photodiode is converted to current. The responsivity (output current divided by the incident radiation power) for the AXUV device is shown below.



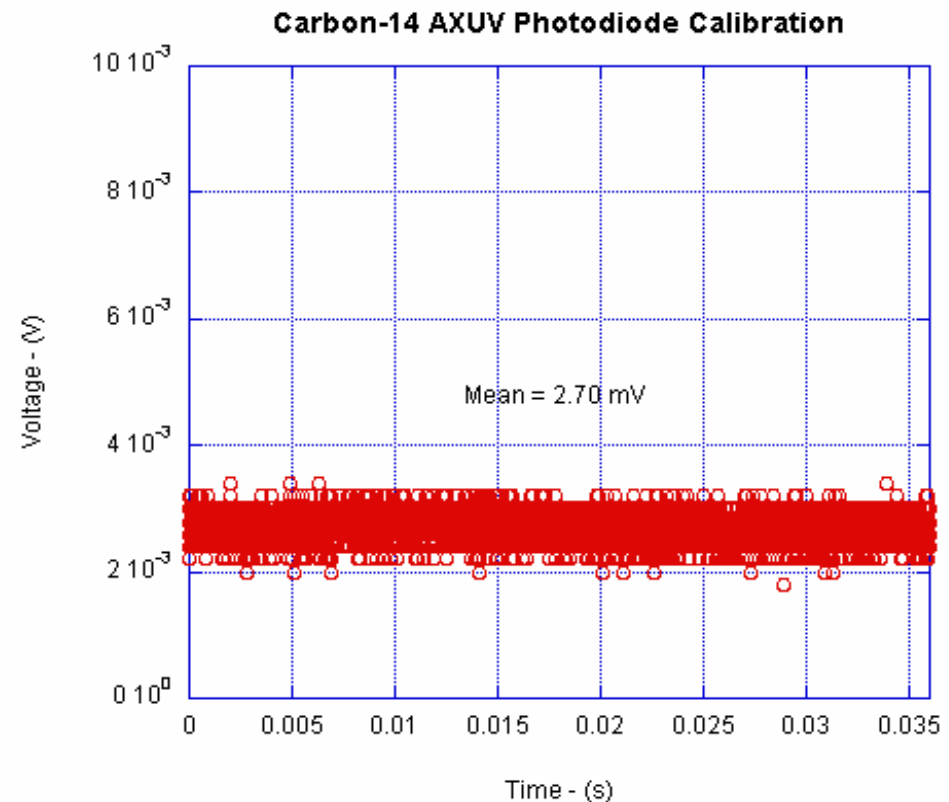


Calibration - Projection

Parameter	Symbol	Units	Value
Activity	A	mCi	7.5
Activity	A	decays/sec	2.78×10^8
Average Beta Energy	E_β	keV	49.5
Average Beta Energy	E_β	J	7.93×10^{-15}
Detector Surface Area	A_D	cm^2	1.0
Source Diameter	D_S	in.	2.75
Source Surface Area	A_S	cm^2	38.3
Power Delivered to the Detector	$P_D = A \cdot E_\beta \cdot A_D \cdot \frac{1}{A_S}$	nW	57.5
Responsivity for ^{14}C Betas	\mathfrak{R}_{C14}	A/W	0.244
Oscilloscope Input Resistance	R_I	Ω	10^6
Projected Oscilloscope Voltage	$V_{Os} = R_{C14} \cdot P_D \cdot R_I$	mV	14.0

Calibration – Results are consistent with a sensitivity of .03 A/W, somewhat lower than mfg predication

- Open Chamber, Lights Out
- 2.70 mV Measured (vs. 14 predicted)
- Glass Layer on Source?

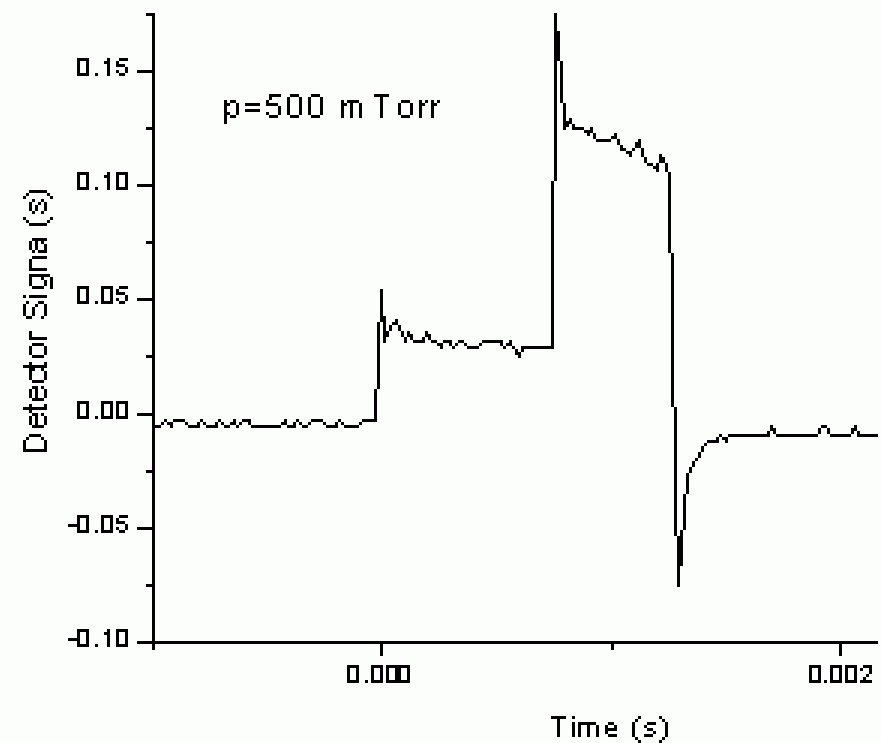
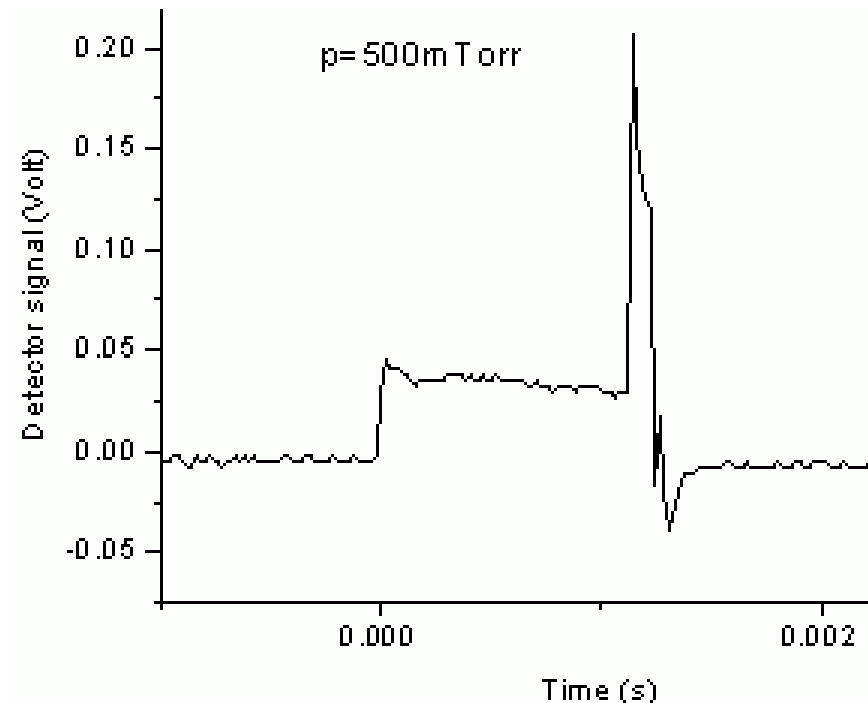




Experiments confirm unique large xray yields during discharge operation.

- At GD operating voltages < 2 kV, very small x-ray yields are expected due to classical Bremsstrahlung.
 - Detector views cathode where ion, not electron bombardment dominates.
 - Ion bombardment induced bremsstrahlung (x-rays) yield at these energies are virtually negligible.
- In contrast, quite significant x-ray yields are observed.
- Most striking: > 600 eV x-rays obtained with only a 300 V discharge. This can not be explained by a classical mechanism such as Bremsstrahlung, suggesting a nonlinear collective phenomenon.

X ray Emission recorded with filtered solid state detector indicates peak emission around $p=500$ mTorr $V=250$ V $I=2$ A for a Ni cathode. Note the delay time of \sim msec before onset of xrays! X-rays are > 600 eV with 250 V discharge!





Comments

- X-ray energy $>$ discharge voltage can not be explained classically
- Delay time before onset appears to be associated with D diffusion into localized sites prior to desorption
- Intensity and efficiency inferred from detector calibration results and geometrical factors discussed next.



Estimates of intensity and efficiency

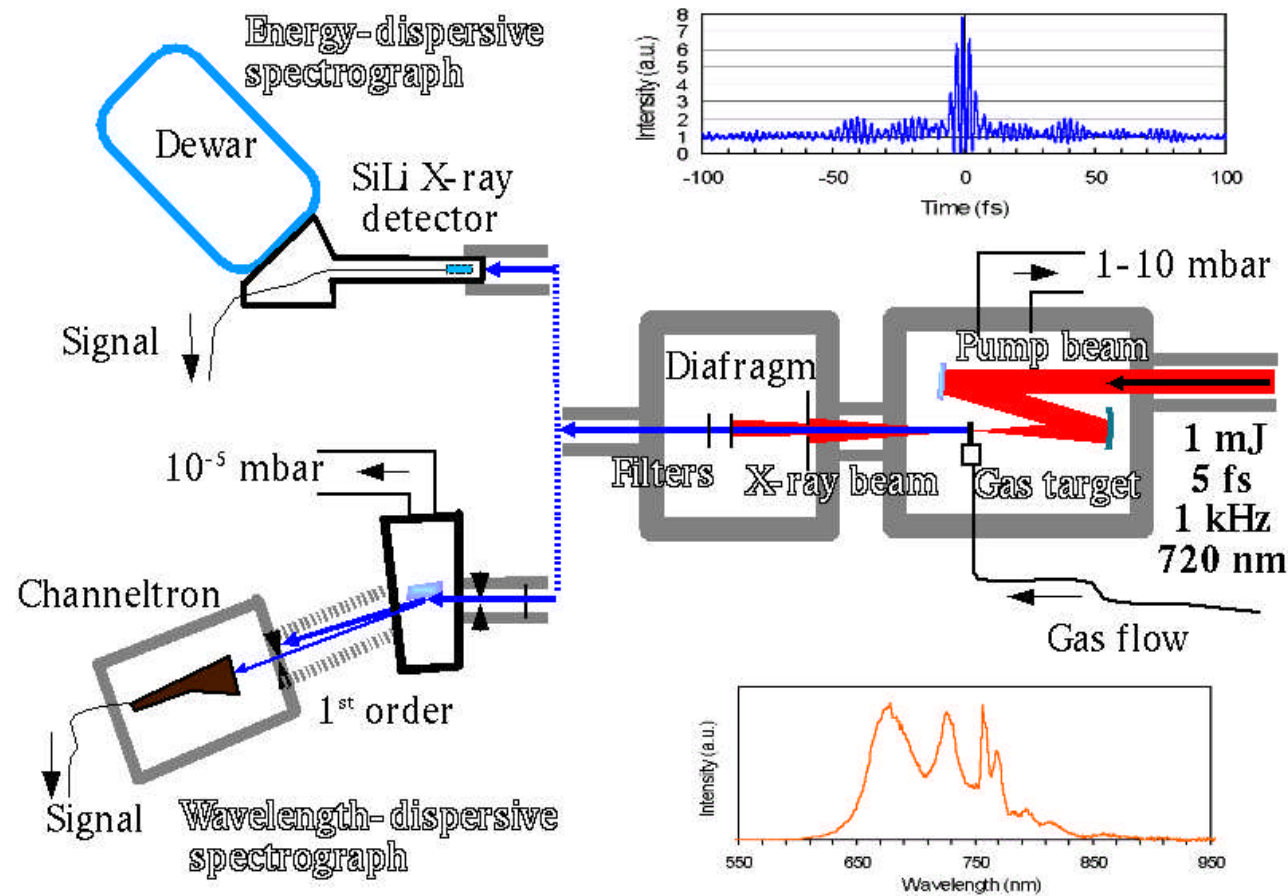
- Assumptions/Values:
 - AXUV photodiode responsivity = 0.270
 - Beryllium filter transmission fraction = 0.75
 - Fraction of the total x-rays escaping through the hole in the plasma-confining glass tube = 0.05
 - Input Power = 375 W, for 1 ms = 0.38 J.
- Calculated xray intensity/efficiency (averaged for 3 measurements):
 - Xray power out = 13.4 mW
 - Intensity = 13.4 mW/cm² (1 cm² Pd target)
 - Xray pulse duration = 0.263 ms
 - Spatial dose per pulse = 3.3 μJ/cm²
 - Efficiency = 8.9×10^{-4} %



Theoretical model

- Directed at explanation of intense emission from glow discharge despite relatively low power density via D bombardment ($\sim \text{kW}/\text{cm}^2$) on target surface
- Preferential loading in dislocation loops and localized ablation over angstrom diameter core (see later figure) results in ultra high local power density.
- Resulting local power flow is comparable with recent coherent emission obtained by others using a ps pulse IR laser and broad surface powers of $10^{17} \text{ W}/\text{cm}^2$ (J. SERES et al., *Nature* 433, 596 (10 February 2005).)

Present mechanism is related to that for --1.3 keV X-ray lasing induced by powerful fs IR-laser hitting He-jet target (J. SERES et al., *Nature* 433, 596 (10 February 2005);





Time sequence- Pulsed GD case

- Pulsed high flux bombardment loading builds up D density and creates dislocations
- D diffuses to dislocations building up high density localized state
- High velocity deloading of localized states produces shock high harmonic generation and xray emission.



The D desorption from small diameter dislocation loops in Pd target results in very large local power flux \sim powerful fs pulsed laser.

- Discharge loading of Pd target occurs at about 2 kW/cm²
- At high surface temperature $T=1940$ K, D escape velocity is $\sim E_d = 0.17$ eV, $v_d = 4 \times 10^5$ cm/s;
- Deuterium flux toward the surface in the deuteron stopping range layer ($E_d \sim 2$ keV, $R_s \sim 15$ nm): $\Phi_d = 1/3 n_d v_d \sim 10^{29}$ cm⁻²-s⁻¹ at $n_d \sim 2 \times 10^{23}$ cm⁻³;
- Assuming D⁺ escapes through the active sites at the Pd-surface (dislocation cores), the local power density is: $S_{eff} = S(dis) \times N_d$. $S_{eff} \sim 10^{-6}$ - 10^{-5} , then
- Then associated localized power: $P_{eff} = \Phi_d \times E_d / S_{eff} \sim 10^{14} - 10^{16}$ W/cm²
- *\sim short pulse IR laser powers.*
- D-diffusion is a coherent process similar to laser beam in fs pulse laser. Both can generate high order harmonic generation.
- **Estimated X-ray quanta:** $h\nu = U_e + 3.2 W_p \sim 1.5$ keV
(Here U_e – is a LII ionization potential, W_p – ponderomotive potential. At $U_e = 460$ eV, $W_p \sim 300$ eV, corresponding to D escape at $P_{eff} \sim 10^{15}$ W/cm².)
- Expected duration of individual X-ray pulses from the Pd-cathode : $\tau = R_s / v_d \sim 4 \times 10^{-12}$ s.

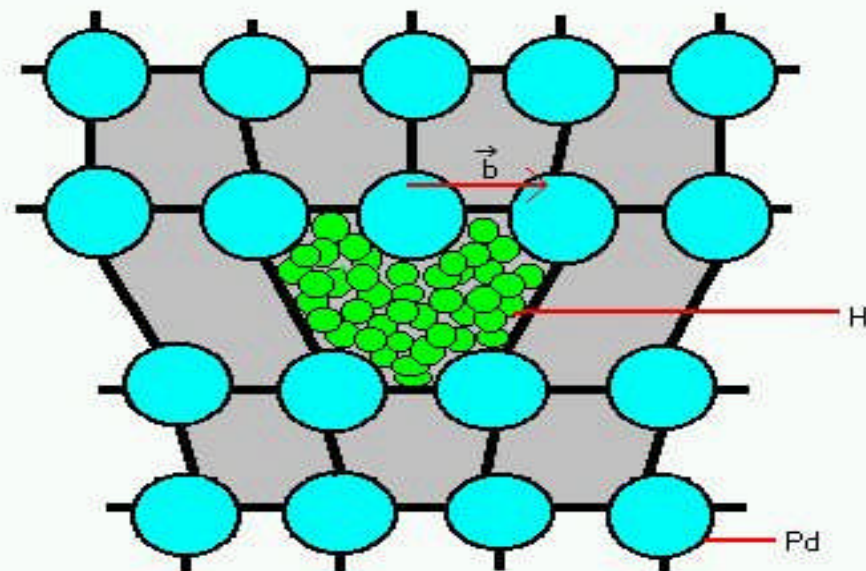
Supporting evidence -- Close-up of a damaged plastic target in Karabut exps-- note the holes appear to be from beamlets.



Independent evidence for localized clusters

Squid measurements on Pd targets have confirmed dislocation loop loading with ultra-high density of deuterium-clusters which form a local superconducting state. [Lipson, et al., J of Physics of Condensed Matter: "Emergence of a High Temperature Superconductivity in Hydrogen Cycled Pd compounds as an Evidence of Super-dense H/D Sites"]

Schematic of edge dislocation core in Pd with Hn-condensed hydrogen phase



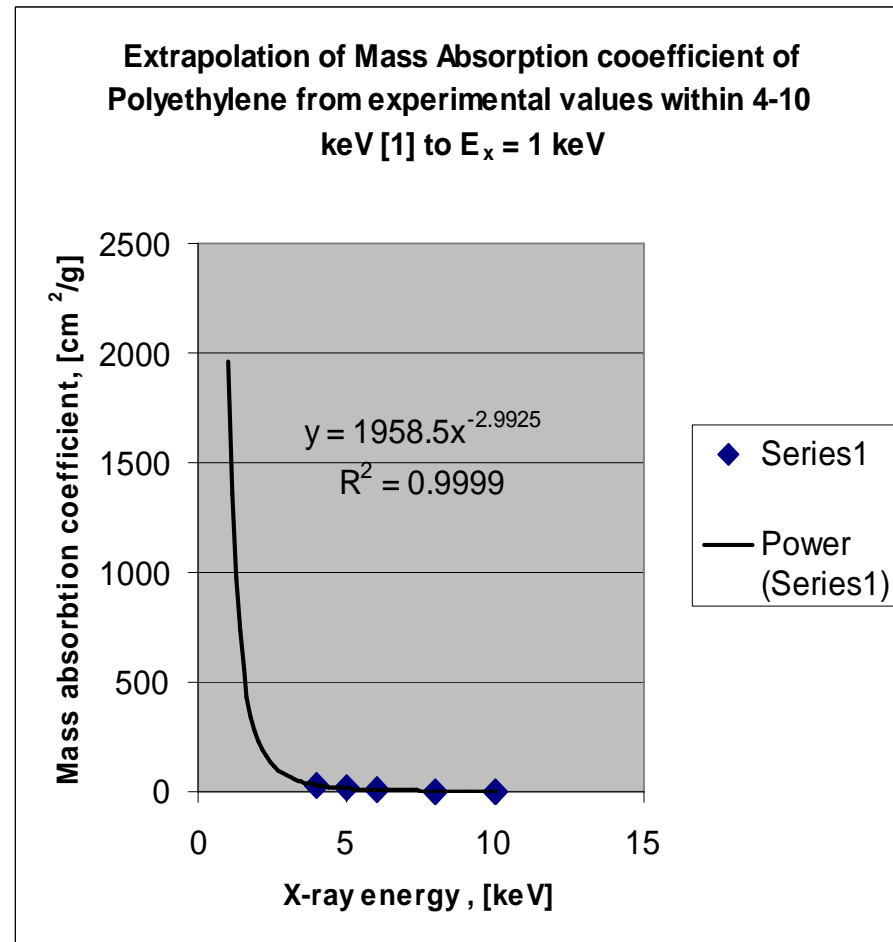
$\text{Pd} [1\bar{2}1]$
 $\vec{b} [101] = 2.75 \text{ \AA}$
ICCF- 12 2005



Auxiliary Experimental verification of desorption theory

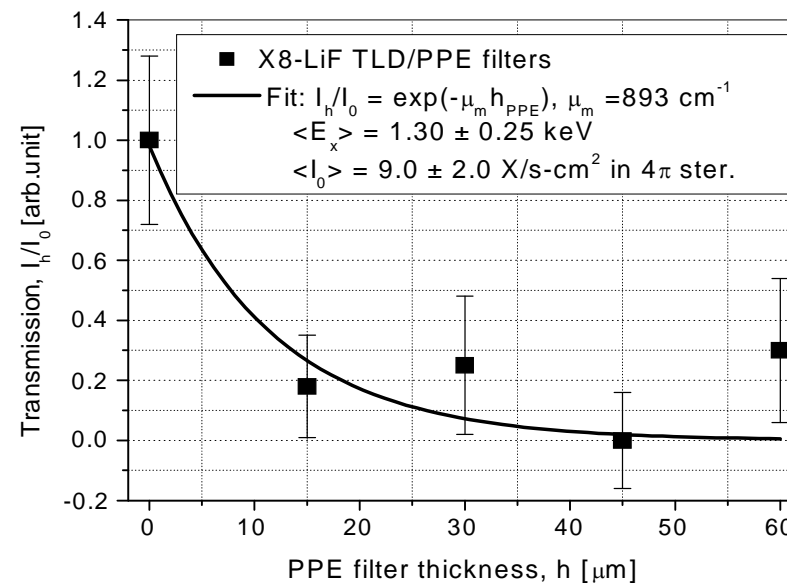
- Experiments were carried out during exothermic deuterium desorption from Pd:Dx cathodes loaded by electrolysis.
- Cathodes were manufactured from the Pd foil used for Glow discharge experiments.
- TLD detection was performed after deuterium loading of the cathode by electrolysis ($J=10 \text{ mA/cm}^2$) suggesting formation of beta phase with $x = \text{D/Pd} \sim 0.7$.
- The deuterium was evolved from the PdDx cathode in spontaneous regime at room temperature.
- A set of TLD with Polypropylene (PPE) filters of 0- 60 μm thick were used for soft X-ray detection.
- The soft X-ray attenuation properties at very low X-ray energy were extrapolated below 4 keV from existing data for polyethylene (PE), which is very similar to PPE.

Filter attenuation vs. E





The average X-ray energy was found to be 1.30 ± 0.25 keV





Comparison to GD results

- The intensity of these X-rays during spontaneous D-desorption at room temperature is about 10-11 orders of magnitude lower than that in GD experiments.
- This is consistent with the lower D fluxes and much lower temperature (i.e. lower exhaust power) in the spontaneous room temperature desorption experiments compared to the pulsed GD experiment.



Conclusions – desorption exps

- The TLD technique can be successfully employed in soft X-ray measurements even at very low intensities.
- The energy of X-ray quanta emitted during spontaneous D-desorption from Pd at room temperature ($E_d \sim kT$) is very close to that emitted during deuteron bombardment of Pd cathode at higher deuteron energy ($300 < E_d < 2000$ eV).
- The last observation supports the mechanism of high order harmonic generation, and suggests the crucial role of D-desorption (resulting in a shock wave generation) during GD deuteron bombardment of cathodes with high hydrogen solubility (e.g. Ti and Pd).



Conclusion – Initial studies confirm anomalous xray emission during ion bombardment.

- Discharge chamber designed and built
- Pulsed power unit designed and operational
- Diagnostic techniques developed
- Initial x-ray measurements confirm anomalous emission associated with dynamic D loading/deloading
 - > 600 eV xrays despite 250-300 eV discharge.
- Theory is based on a high local power density due to desorption of D-clusters from localized dislocation loops.



- For further information contact

George H. Miley

ghmiley@uiuc.edu

217-333-3772

Fusion Studies Laboratory

103 S. Goodwin Ave. MC-234

100 Nuclear Engineering Lab

Urbana, Illinois 61801 USA

Acknowledgements: work supported by the AFRL, JTO
Office, Albuquerque, NM